Active control of vortex–wall interactions

Petros Koumoutsakos[a)]
CTR, NASA Ames 202A-1, Moffett Field, California 94035

(Received 8 January 1997; accepted 28 August 1997)

A new simple and efficient methodology is presented for the active control of vortical wall bounded flows. The method is based on sensing of the wall pressure and the calculation of the wall vorticity flux. This information is used to determine explicitly the amount of unsteady, spatially varying mass transpiration, used as an actuating mechanism, necessary to achieve a desired wall vorticity flux. The present scheme is based on the physical mechanism of vorticity generation at solid boundaries. It has the advantage of implementing quantities that can be measured and manipulated at the wall, in computations as well as in experiments. It is shown to reproduce efficiently phenomena previously attained using off-wall information. An active control methodology is outlined and the practical implementation of the present scheme is discussed. © *1997 American Institute of Physics.* [S1070-6631(97)03712-4]

I. INTRODUCTION

The control of vortical flows is gaining significance in the design of aeronautical and marine structures. While passive devices have been used effectively in the past, active control strategies have the potential of allowing a leap in the performance of future configurations. The efficiency of control schemes is strongly dependent on the development of accurate flow models that can be devised using information that is available not only from numerical solutions of the governing Navier–Stokes equations but also can be measured experimentally. In that context it is desirable to construct adaptive control schemes using information that can be measured at the wall.

The objective of this study is to propose an efficient methodology for the adaptive control of vortical, wall bounded flows. It is based on the sensing and manipulation of the wall vorticity flux. The wall pressure is sensed at the wall and the wall vorticity flux is calculated. Blowing/suction at the wall is the actuating mechanisms and its strength may be calculated explicitly by formulating the mechanism of vorticity generation at a no-slip wall.

It is well known (Andreopoulos and Agui,[1] referred to as AA from here on), that one may obtain the wall flux of all three vorticity components as a function of time by measuring the instantaneous pressure at the wall and calculating its gradient. Wall pressure fluctuation measurements are often reported in the literature[2] and have revealed a strong coupling between the vortical structures near the wall and the pressure field on the wall. Similar observations have been made[3] in flow fields obtained in direct numerical simulations of wall bounded flows. However, measurements of pressure gradients at a wall are not common. An exception is the work of AA. They use high-frequency response transducers to measure fluctuating wall pressure gradients and then compute the vorticity flux in a two-dimensional turbulent boundary layer. Their measurements demonstrated the significance of vorticity flux in describing near wall processes. They made an attempt to correlate vorticity flux signals with physical phenomena such as bursting-sweep processes in the boundary layer. They observed that fluid acquires or loses vorticity at the wall during rather violent events followed by periods of small fluctuations. During these events they observed a predominant orientation at 45° for the wall vorticity flux, implying an equal vorticity flux for the streamwise and the spanwise vorticity components. This may be linked with the observations of Orlandi and Jimenez,[4] who studied the role of spanwise vorticity in the redistribution of streamwise vortices and the formation of streaks of high and low skin friction in the boundary layer.

AA demonstrated that the major contributions to the vorticity flux come from the uncorrelated part of the pressure signals, at two adjacent locations, which contain a wide range of vortical scales. As the degree of correlation is smaller between the small scales their contribution to the vorticity flux is more pronounced. This imposes a severe requirement on the spatial resolution of the pressure gradients/vorticity flux measurements. Practical applications[5] (such as flight conditions, with $U_\infty = 300$ m/s, $u_\tau = 10$ m/s, $\nu = 3\times10^{-5}$ m^2/s) would require actuators and sensors with sizes in the order of 50 μm and actuator frequencies of 1 MHz. Recent advances in micropressure sensor fabrication technology[6] give us an opportunity to overcome these difficulties. Löfdahl *et al.*[7] presented measurements in a two-dimensional flat plate boundary layer with a resolution of eddies with wave numbers less than ten viscous units using microscopic silicon pressure transducers. It appears that using this new technology one may be able to describe in detail physical processes in terms of the flow vorticity and the wall vorticity flux.

The role of the vorticity flux from oscillating walls as a mechanism for control of unsteady separated flows was discussed by Wu, Wu, and Wu.[8] They concluded that wall oscillations can produce a mean vorticity flux that is partially responsible for phenomena of vortex flow control by waves. Gad-El-Hak[9] has shown that the vorticity flux can be affected by wall transpiration as well as by wall–normal variation of the kinematic viscosity (ν) as a result of surface heating, film boiling, cavitation, sublimation, chemical reaction,

[a)]Also at the 1FD, ETH Zentrum, Zürich, CH-8092, Switzerland.

 1070-6631/97/9(12)/3808/9/$10.00

wall injection of higher/lower viscosity fluid, or in the presence of a shear thinning/thickening additive.

However, these works do not provide us with an explicit formulation for the actuator strength necessary to induce a desired vorticity flux at the wall. In that direction, recently Lee, Kim, Babckock, and Goodman[10] used nonlinear neural networks to obtain a simple expression for the wall blowing and suction needed to reduce the skin friction of turbulent channel flow. In this paper we propose the use of vorticity flux for effective, adaptive control mechanisms in wall bounded flows. For a general fluid material the wall vorticity flux may be affected by appropriately selecting the type, magnitude, and location of the controlling devices so as to modify the fluid stresses near the wall. For the present scheme using a formulation based on Lighthill's[11] conceptual model of vorticity generation at the wall, we obtain in closed form the magnitude of the blowing/suction necessary to manipulate the vorticity field. The present control scheme relies on information that can be obtained experimentally as well as computationally. It is applied to the model problem (Choi, Moin, and Kim[12]—referred to as CMK from here on) of a vortex dipole interacting with a wall. It is shown that the present strategy, using wall only information, reproduces efficiently phenomena that have been obtained previously using off-wall information.

II. THE WALL–VORTICITY FLUX

In wall bounded flows, the tangential velocity of fluid elements relative to the wall establishes velocity gradients. With the definition of vorticity ($\boldsymbol{\omega}$) as the curl of velocity ($\boldsymbol{\omega}=\boldsymbol{\nabla}\times\mathbf{u}$), this may be equivalently described in terms of the vorticity that is acquired by the fluid elements near the wall. Lighthill[11] envisioned the wall as a system of sources and sinks of vorticity. He drew an analogy between the way vorticity is produced at the wall and enters the flow and the way temperatures are established near a heat conducting boundary.

Following Hornung[13] we identify the *diffusive vorticity flux tensor at the wall* as

$$J_w=-(\nu\ \boldsymbol{\nabla}\boldsymbol{\omega})_w, \tag{1}$$

where ν is the kinematic viscosity of the fluid and the subscript w denotes quantities measured at the wall.

The normal component of the diffusive vorticity flux tensor is defined as the wall vorticity flux,[14]

$$\boldsymbol{\sigma}=-(\nu\mathbf{n}\cdot\boldsymbol{\nabla}\boldsymbol{\omega})_{\mathbf{W}}, \tag{2}$$

where $\boldsymbol{\omega}$ is the vorticity and $\mathbf{n}$ is the outward normal at the wall. In the rest of this work we consider for simplicity a Cartesian coordinate system and flow over a flat wall identified with the xOz plane (Fig. 1) with a unit normal $\hat{j}$. The vorticity flux is then expressed as

$$\boldsymbol{\sigma}=-\left(\nu\frac{\partial\boldsymbol{\omega}}{\partial y}\right)_{\mathbf{W}}. \tag{3}$$

Hornung[13] has presented a formula for the local vorticity flux for a general fluid material:

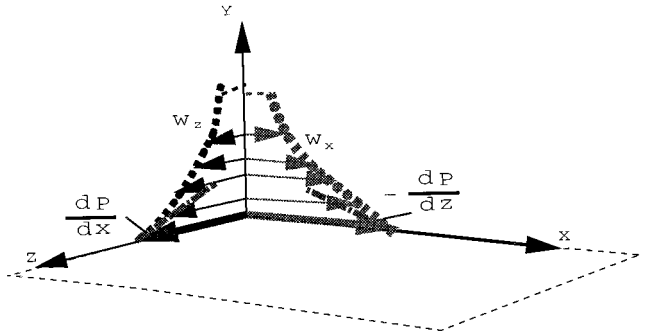

FIG. 1. Definition sketch.

$$\boldsymbol{\sigma}=-\hat{j}\times\left(\frac{d\mathbf{V}_w}{dt}+\frac{(\boldsymbol{\nabla}p)_w}{\rho_w}\right)-\frac{1}{\rho_w}\hat{j}[\hat{j}\cdot(\boldsymbol{\nabla}\times\tau_w)]+\frac{1}{\rho_w}\hat{j}\times\begin{bmatrix}\dfrac{\partial\sigma_x}{\partial x}\\ \dfrac{\partial\sigma_z}{\partial z}\\ 0\end{bmatrix}, \tag{4}$$

where $\mathbf{V}_w(t)$ is the local wall velocity, ρ_w is the local fluid density, τ_w is the shear stress tensor, and σ_x, σ_z the components of the normal stress components along the wall. For an incompressible viscous flow over a stationary wall, the vorticity flux is directly proportional to the pressure gradients, as Eq. (4) reduces to

$$\nu\left(\frac{\partial\omega_x}{\partial y}\right)_w=\frac{1}{\rho}\left(\frac{\partial p}{\partial z}\right)_w \quad\text{and}\quad -\nu\left(\frac{\partial\omega_z}{\partial y}\right)_w=\frac{1}{\rho}\left(\frac{\partial p}{\partial x}\right)_w, \tag{5}$$

where p is the pressure and ω_x and ω_z are the streamwise and spanwise vorticity components (Fig. 1). Note, that the flux of the wall normal vorticity, ω_y, may be determined from the kinematic condition ($\boldsymbol{\nabla}\cdot\boldsymbol{\omega}=0$) as

$$-\left(\frac{\partial\omega_y}{\partial y}\right)_w=\left(\frac{\partial\omega_x}{\partial x}\right)_w+\left(\frac{\partial\omega_z}{\partial z}\right)_w. \tag{6}$$

The present control scheme is based on the measurement and control of the spanwise and streamwise vorticity flux components, which can be obtained as a function of time by measuring the instantaneous pressure at the wall and calculating its gradient.

A. Vorticity flux induced by blowing and suction at the wall

We proceed to describe our methodology by considering two-dimensional configurations. The present analysis and the results discussed herein are readily extendable to three-dimensional flows.

Following Lighthill,[11] the generation of vorticity at the wall is considered as a fractional step algorithm. The algorithm considers the evolution of the vorticity field in discrete viscous and inviscid substeps. The enforcement of the no-slip boundary condition provides a link between the inviscid and viscous description of the flow in terms of the vorticity field.

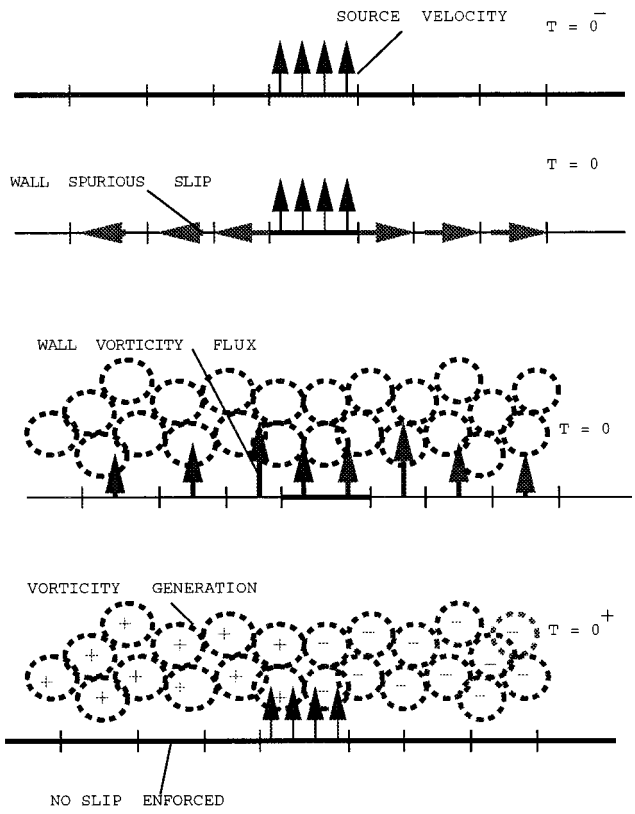

FIG. 2. Slip cancellation algorithm. The slip velocity and wall vorticity flux are averaged over wall segments.

More specifically, during the first substep the vorticity field evolves inviscidly, inducing a spurious slip velocity (or equivalently a vortex sheet) at the boundary. The vortex sheet at the boundary and the vorticity field determine the evolution of the whole flow field. At the following substep the no-slip boundary condition is enforced. The vortex sheet enters diffusively into the flow, eliminating the spurious velocity at the wall and resulting in vorticity creation at the boundary.

To illustrate this process consider the generation of vorticity over a wall due to the instantaneous blowing at one segment of the wall (Fig. 2). According to Lighthill's model, there is a slip velocity at the wall for an instant. A simple calculation shows that over an elementary wall segment δs we may calculate a circulation of $\delta\Gamma = U_{\text{slip}}\ \delta s$. The spurious slip velocity U_{slip} may be easily determined from inviscid flow theory and at each location it is proportional to the inverse distance from the source. This spurious slip velocity is then nullified via the diffusive generation of vorticity at the wall so that the no-slip boundary condition is enforced. The amount of circulation that enters the flow over each time step δt, over each segment, is then $\delta\Gamma$, and it is related to a vorticity flux as $\delta\Gamma = \nu\ \partial\omega/\partial y\ \delta t\ \delta s$. Thus, the instantaneous vorticity flux at each location over the wall due to the instantaneous blowing is expressed as

$$\nu\left(\frac{\partial\omega}{\partial y}\right)_w = -\frac{U_{\text{slip}}}{\delta t}. \tag{7}$$

We consider now a system of sources/sinks at the wall, of strength q_j that are distributed uniformly over a panel of size d_j, centered at locations x_j', $j=1,2,3,\ldots, N$. The induced tangential velocity at point x_i on the wall and the corresponding vorticity flux may be determined as

$$\nu\ \delta t\ \frac{\partial\boldsymbol{\omega}}{\partial y}(x_i) = \sum_{j=1}^{N}\ \frac{q_j}{2\pi}\int_{-d_j/2}^{d_j/2}\frac{ds}{x-s}, \tag{8}$$

where $x = x_i - x_j'$.

It is clear that via the present formulation the velocity gradients at the wall induced by the source/sink actuators may be determined as well and, ultimately, they can be used to affect the wall shear stresses. Moreover, similar expressions relate the vorticity flux at a location on the wall with the tangential acceleration of wall elements. Hence, the formulation described herein may be easily extended to control problems where the actuating mechanism is provided by the local deformation of the body.

II. AN ADAPTIVE CONTROL STRATEGY

For the purposes of our control scheme we consider a series of vorticity flux (or equivalently pressure gradient) sensors on the wall at locations x_i, $i=1,2,3,\ldots, M$. Using the formulas described above, we can explicitly determine the actuator strengths necessary to achieve a desired vorticity flux profile at the wall, at a time instant k, by solving the linear set of equations:

$$Bu_k + X_{k-1} = D_k, \tag{9}$$

where $D_k = ((\partial\omega^k/\partial y)(x_1),(\partial\omega^k/\partial y)(x_2),\ldots,(\partial\omega^k/\partial y)\times(x_M))$ is an $M\times 1$ vector of the *desired* vorticity flux at the sensor locations, $X_{k-1} = ((\partial\omega^{k-1}/\partial y)(x_1),(\partial\omega^{k-1}/\partial y)\times(x_2),\ldots,(\partial\omega^{k-1}/\partial y)(x_M))$ is an $M\times 1$ vector of the *measured* vorticity flux at the sensor locations and $u_k = (q_1^k(x_1'),q_2^k(x_2'),\ldots,q_N^k(x_N'))$ is an $N\times 1$ vector of the source strengths at the actuator locations, B is an $M\times N$ matrix whose elements B_{ij} are determined by evaluating the integrals in Eq. (8) as

$$B_{ij} = \frac{1}{2\pi}\,\text{Log}\,\frac{|x_j' - x_i - d_j/2|}{|x_j' - x_i + d_j/2|}. \tag{10}$$

Matrix B is a sparse matrix and when large numbers of sensors and actuators are employed one may use multipole expansions to reduce the computational cost. Furthermore, if the relative locations of the sensors and actuators remain constant, matrix B needs to be inverted only once, thus minimizing the computational cost of the method. Note that the location of sensors and actuators may be selected in such a way that the matrix B is *symmetric, positive definite*. By setting $D_k = (1+\alpha)X_k$, the solution of the above system of equations then implies the minimization of the functional,

$$P(u_k) = \frac{1}{2}\,u_k^T B u_k - \alpha u_k^T X_k. \tag{11}$$

The present technique gives us flexibility over the specific constraints that we wish to impose on the actuator strengths. Practical considerations may impose that the control is per-

formed only by jet-like actuators, $q_j \geqslant 0$, $j=1,...,N$ or that the blowing and suction configuration should result in a net zero mass flux;

$$\sum_{j=1}^{N} q_j = 0. \tag{12}$$

Such constraints may be easily incorporated in the above scheme by appropriately adjusting matrix B. A square matrix is always possible by accordingly modifying the number of sensors and actuators. In the present example the zero mass constraint was implemented so that $B_{Mj}=1$, $j=1,...,N$.

Sensors and actuators are not in the same locations. The simplicity of the present scheme allows for a number of different placements of sensors and actuators. Moreover, it allows for the *active* selection of the optimal locations (e.g., for drag reduction) by suitable optimization algorithms. Here we chose the locations of sensors and actuators to be collocated. This includes cases where the sensors and actuators are separated by an uncontrolled (small) segment of the wall and cases where they are adjacent to each other. Physically this may be understood as a favorable situation, as the sensors are able to sense the vorticity field induced by the actuators allowing for the control scheme to suitably compensate for it.

III. CONTROL OF VORTEX DIPOLE INTERACTIONS WITH A WALL

To illustrate the effects of the present control strategy on vortex–wall interactions, we consider the idealized situation of a two-dimensional vortex dipole interacting with a wall. This model has been used in the past by CMK and it allows us to compare our scheme with previous well-established control strategies and draw some conclusions as to its efficiency.

We consider a Lamb's vortex dipole of radius R, traveling with velocity U. The Reynolds number of the initial vortex dipole is defined as $\mathrm{Re}=UR/\nu$, and in all simulations discussed herein $\mathrm{Re}=400$ and the vortex is initially located at a distance of $2.5R$ above the wall. For the simulations presented herein we employ a fast high resolution viscous vortex method.[15] No symmetry constraint is imposed on the evolution of the vorticity field, the time step is chosen as $\delta t=0.01$, and the size of the Lagrangian vortex particles is chosen as $\epsilon^2=0.0002$. A maximum of 200 000 Lagrangian computational elements were used for these simulations. For more details on the implementation of fast viscous vortex methods and the selection of numerical parameters, the reader is referred to Koumoutsakos and Shiels.[16]

The sensors and actuators have a finite size. In our computational experiments we found that the sensed vorticity flux is more accurately described when we calculate its average over a finite segment of the wall and that the finite size of the actuators allows for a more well-conditioned description of the velocity field near the wall. The effect of different actuator and sensor arrangements is assessed by considering here the following four configurations.

Configuration 1a: Sensors of size 0.1, centered at $\pm(0.15+0.4i)$, $i=0,...,5$ and actuators of the same size centered at $\pm(0.05+0.4i)$, $i=0,...,6$.

Configuration 1b: The same as configuration 1a, but with additional sensors of size 0.1 at $\pm(0.35+0.4i)$, $i=0,...,4$ for a total of 22 sensors and additional actuators at $\pm(0.25+0.4i)$, $i=0,...,5$ for a total of 26 actuators.

Configuration 2a: Sensors of size 0.1, centered at $\pm(0.15+0.2i)$, $i=0,...,11$ and actuators of the same size centered at $\pm(0.05+0.2i)$, $i=0,...,12$.

Configuration 2b: The same as configuration 2a, with additional sensors of size 0.1 at $\pm(2.55+0.2I)$, $I=0,...,7$ or a total of 40 sensors. Also additional actuators, of size 0.1, at $\pm(2.45+0.2I)$, $I=0,...,8$ for a total of 42 actuators.

Note that in order to enforce the zero mass flux constraint one needs at least one more actuator than the sensors. Because the present calculations are of a left–right symmetric flow, we enforce symmetry in the blowing/suction magnitude of the actuators. Hence the number of sensors and actuators in all configurations are related by $N/2=M/2+1$.

Representative animations of the simulations discussed in the following section may be found on the worldwide Web (http://www.galcit.caltech.edu/~petros/RESEARCH/dipole.html).

A. Uncontrolled vortex–wall interactions

In Fig. 3 we present contour plots of the vorticity field of the uncontrolled interaction of a vortex dipole with a wall. The vortex dipole propagates toward the wall generating vorticity of opposite sign on its surface. As the primary vortex approaches the wall, it interacts with this secondary vorticity generating two new dipoles that propagate outward ($T=0$ to 1.5). When the initial components of the dipole are far apart, the new dipolar structures are lifted from the wall ($T=1.5-2.0$). The lifted secondary vorticity is weaker than the respective primary vorticity field. Thus, the preferential direction of the new dipoles results in an interaction between the original dipole components so that the vortical structures propagate again towards the wall ($T=2-4$). New secondary vorticity is generated and the process described before is repeated ($T=4-5$). However, due to the action of diffusion, the vorticity field is weakened ($T=5$ to 6) resulting in a quasisteady pattern that is eventually eroded.

The results of the present simulations are in excellent agreement with the results of Orlandi[17] to which the reader is referred for a thorough discussion and quantification of this dipole wall interaction.

B. Control canceling the wall flux

In Fig. 4 and in Fig. 5 we present contour plots of the vorticity field of the controlled interaction of a vortex dipole with a wall. In this type of control we eliminate the vorticity flux at the sensor locations (i.e., set $D_k=0$). The vorticity flux is measured at each instant and at the following time step we appropriately adjust the strength of the actuators by solving

$$Bu_k = -X_{k-1}, \tag{13}$$

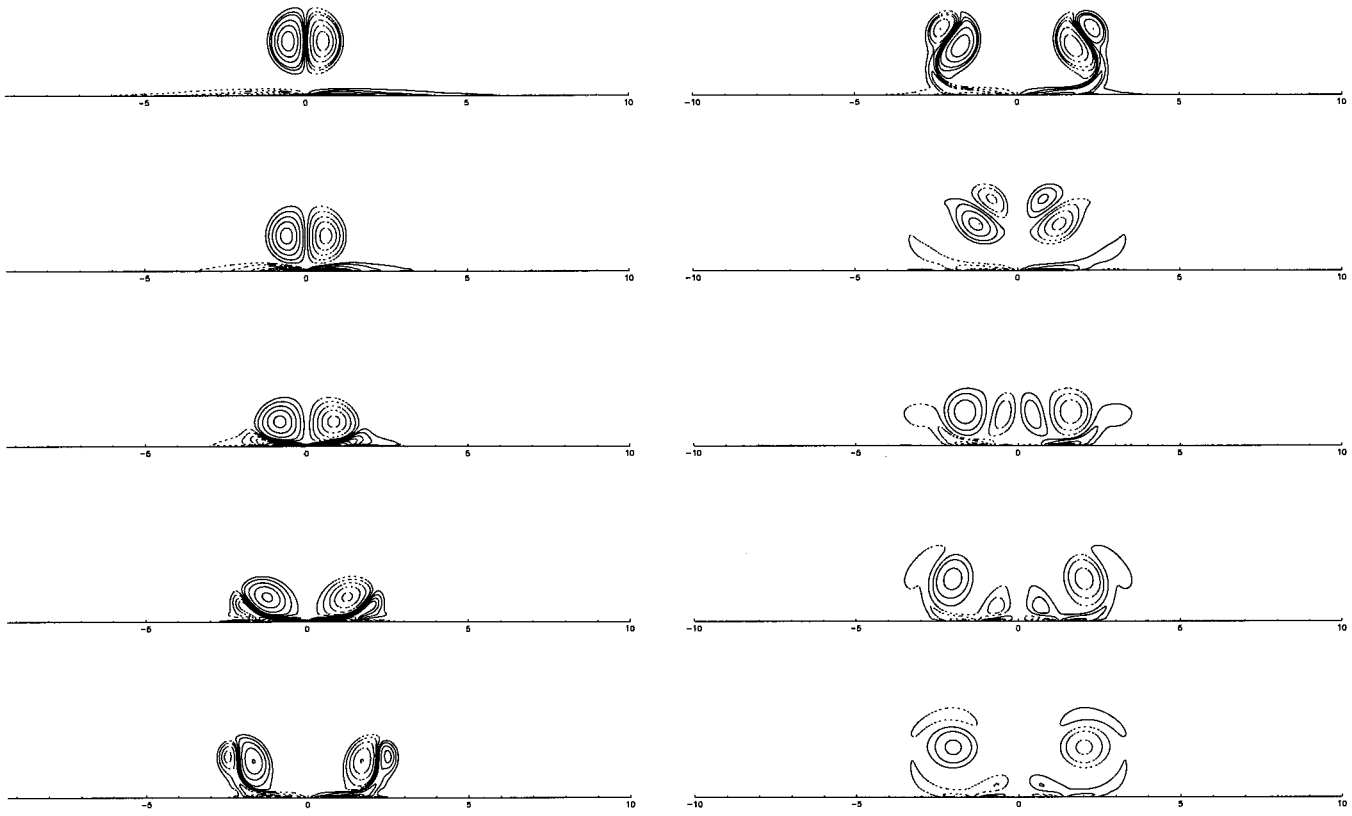

FIG. 3. *Uncontrolled* interactions of a vortex dipole with a wall. Contours at $T=0.0$, 0.2, 0.5, 1.0, 1.5, 2.0, 3.0, 4.0, 5.0, 6.0 (top to bottom, left to right).

for u_k. This scheme may be viewed as an *out-of-phase* control of the vorticity flux.

As the vortex descends toward the wall, the cancellation of the vorticity flux in the sensor locations results in a pattern where sinks are distributed in the middle of the wall. Respective blowing is established in the outer actuators so that the zero net mass flux is enforced (see also Figs. 6 and 7). As the control scheme acts to eliminate the secondary vorticity generated at the wall the primary vortex dipole ''sees'' a permeable wall. At time $T=1.0$ the primary vortex dipole has been drawn into the wall.

We examine here the effect of actuator placement in this type of control, by using the sets of sensors and actuators locations described in configurations 1a and 1b above. Both arrangements result in the suction of the impinging vortex dipole. However, the vorticity field in configuration 1a is more active (Fig. 4), whereas in 1b all vorticity is eliminated from the flow field at the respective stages of the simulation. These differences may be explained by observing that in 1b the locations of sensors and actuators are collocated and adjacent to each other. This allows for the sensors to account for the vorticity field generated by the actuators. As the present control strategy requires the elimination of the vorticity flux at the sensor locations, the actuator strengths are adjusted so that blowing/suction is reduced. On the other hand in configuration 1a the sensors are more distant from the actuators. As the few outer actuators are required to blow strongly to compensate for the suction pattern in the middle in order to enforce the zero net mass flux, they generate a local strong vorticity field that results in the ejection of small vortical structures (Fig. 4). Eventually this field is sensed by the sensors and the actuator strength is diminished progressively.

In Fig. 6 and Fig. 7 we present the distribution of the actuator strengths for time instances corresponding to the vorticity contours shown in Fig. 4 and Fig. 5 respectively. A simple pattern is rapidly established and is qualitatively the same for both configurations. The time invariance of the source/sink patterns at the wall suggests a weak time correlation of the flow induced wall vorticity flux signals. The control scheme identifies the oncoming vortical structures and takes appropriate action to cancel the vorticity flux so that the dynamics of the flow are eventually governed by the dynamics of the actuators.

C. Control enhancing the wall flux

In Fig. 8 and in Fig. 9 we present contour plots of the vorticity field of another type of controlled interaction of a vortex dipole with a wall. In this case the desired vorticity flux is such that the secondary vorticity is enhanced and the lift off, observed in the uncontrolled case, is prevented. To achieve this, we require that the actuator strengths are adjusted so as to maintain the sensed vorticity flux (or equivalently $D_k=2X_{k-1}$) via the solution of the system

$$B\mathbf{u}_k=\mathbf{X}_{k-1}. \tag{14}$$

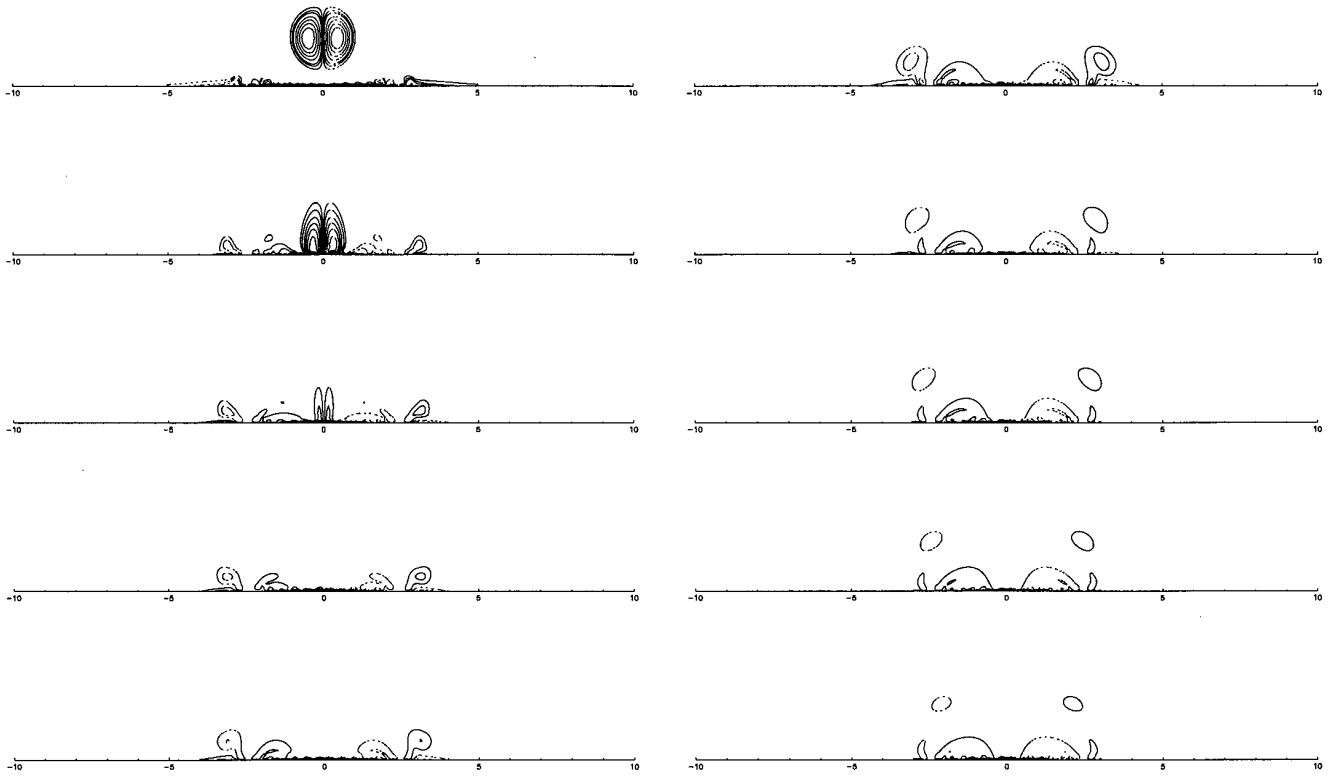

FIG. 4. Configuration 1a: *Controlled* wall–vortex interaction. Contours at $T=0.0$, 0.2, 0.5, 1.0, 1.5, 2.0, 3.0, 4.0, 5.0, 6.0 (top to bottom, left to right).

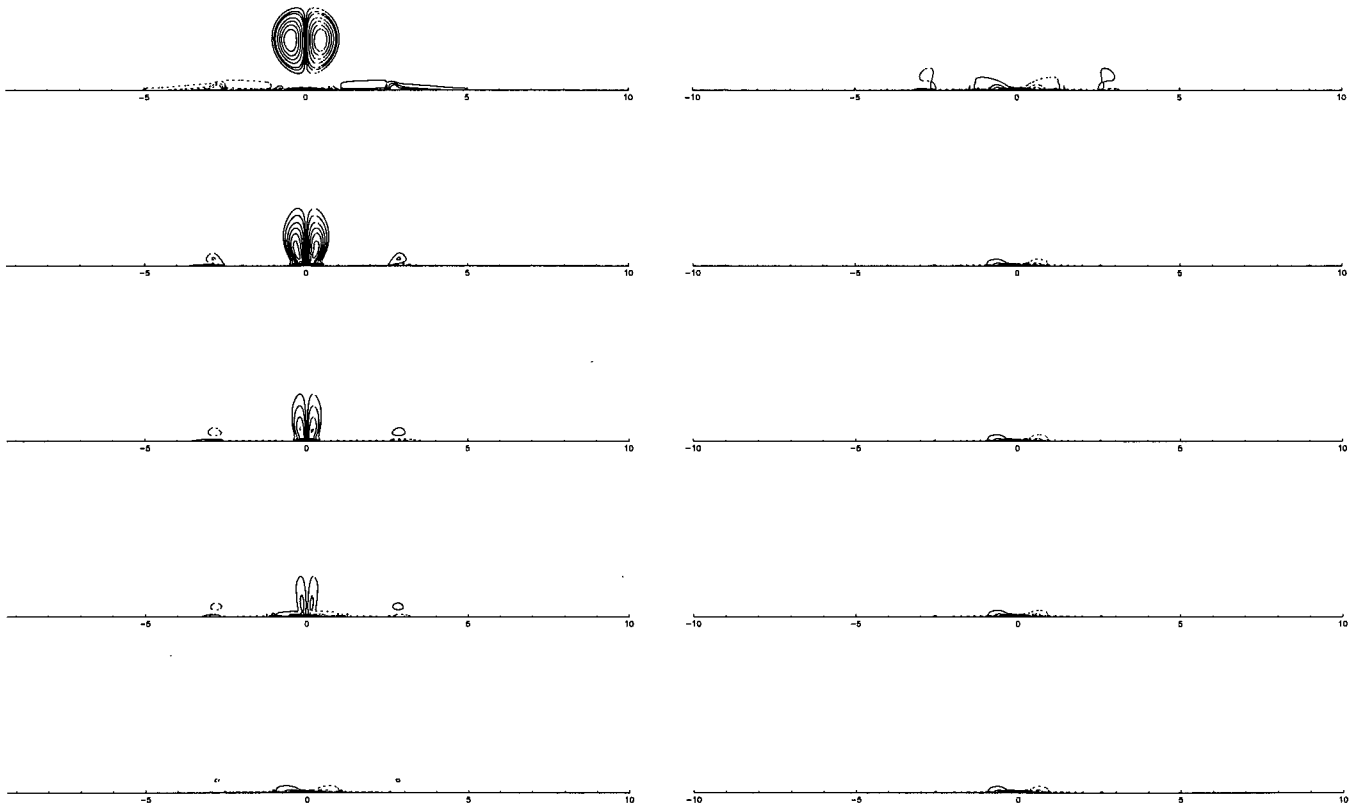

FIG. 5. Configuration 1b: *Controlled* wall–vortex interaction. Contours at $T=0.0$, 0.2, 0.5, 1.0, 1.5, 2.0, 3.0, 4.0, 5.0, 6.0 (top to bottom, left to right).

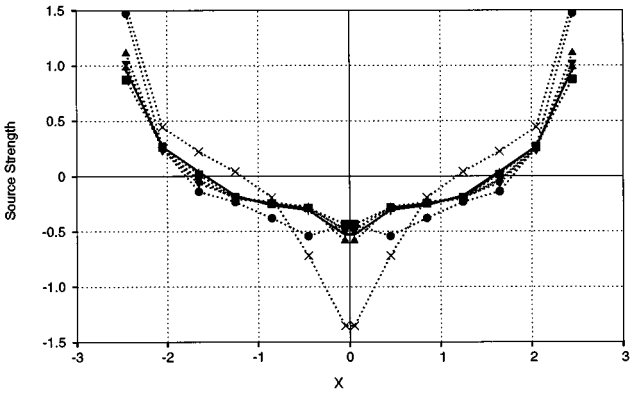

FIG. 6. Configuration 1a: source strengths at times: ●, 0.2; ×, 0.5; △, 1.0; ▽, 2.0; ◇ 3.0; □, 4.0; +, 5.0; —, 6.0.

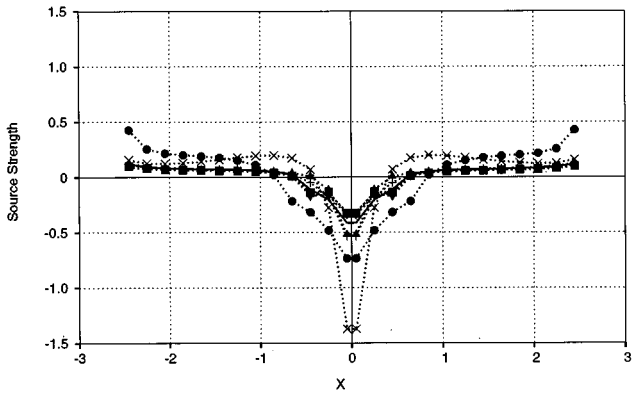

FIG. 7. Configuration 1b. For symbol captions see Fig. 6.

This scheme may be viewed as an *in-phase* control of the vorticity flux.

The vorticity flux induced by the actuators at each time step is enforced to be equal to the vorticity flux induced by the flow at the previous time step. Hence, the control scheme tries to enhance the wall vorticity flux. We consider again two arrangements of sensors and actuators. Using the observations from the previous case in both arrangements, the sensors are adjacent to the actuators. In 2a sensors and actuators extend up to ± 2.50, whereas in 2b they extend out to ± 4.05.

As the vortex dipole approaches the wall, it interacts with secondary vorticity. In this case, the primary vortex components roll on the sheet of secondary vorticity that the actuators try to maintain. Lift off is prevented as the primary vortex components ''surf'' the controlled portion of the wall. The vortical structures eventually lift off outside the controlled region, as the primary vortices have not lost enough of their strength by the act of diffusion. The lift-off process outside the controlled region is affected by the enhancement of the secondary vorticity by the action of the control scheme. For example, compare the last frame in Fig. 8 with the last frame in Fig. 3. In Fig. 10 and Fig. 11 we present the actuator strengths for the two configurations for a series of time instances. Initially the actuator strengths are such that they oppose the descent of the vortex dipole. As the second-

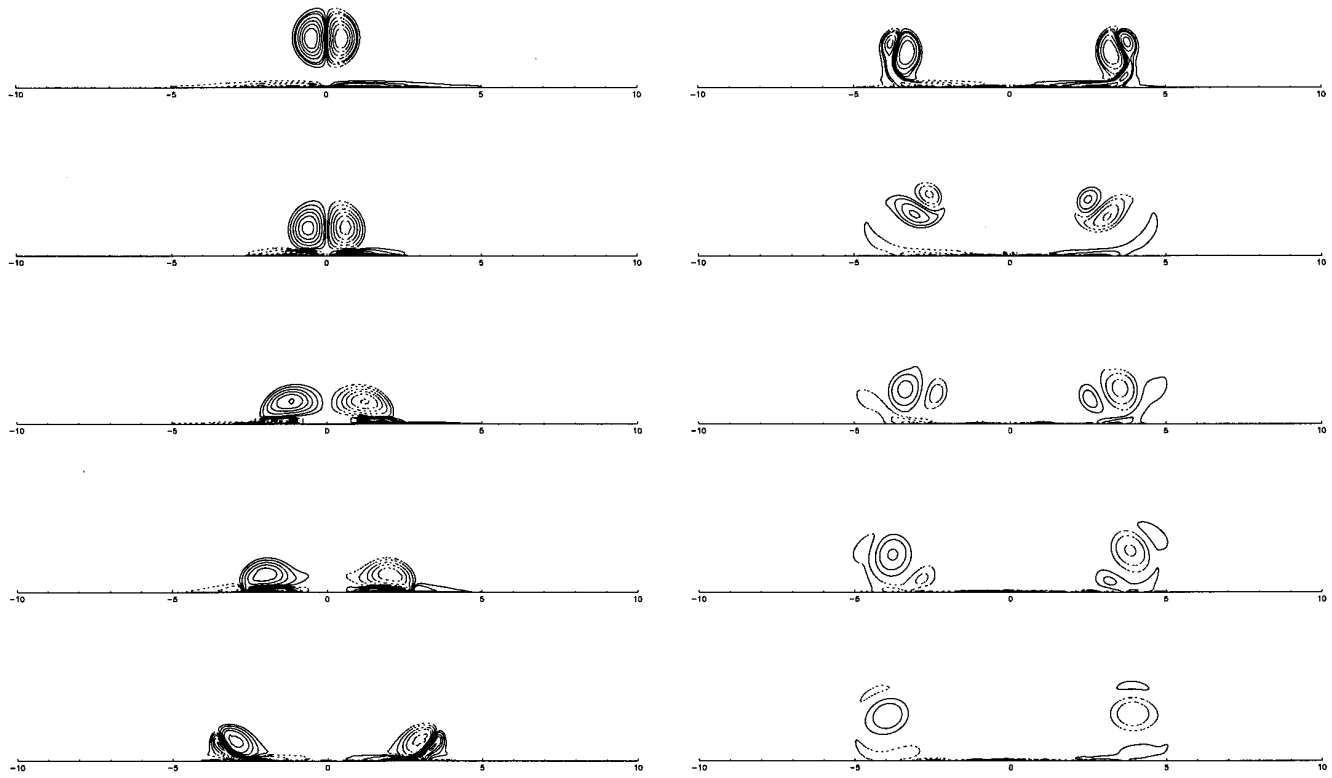

FIG. 8. Configuration 2a: *Controlled* wall–vortex interaction. Contours at $T=0.0$, 0.2, 0.5, 1.0, 1.5, 2.0, 3.0, 4.0, 5.0, 6.0 (top to bottom, left to right).

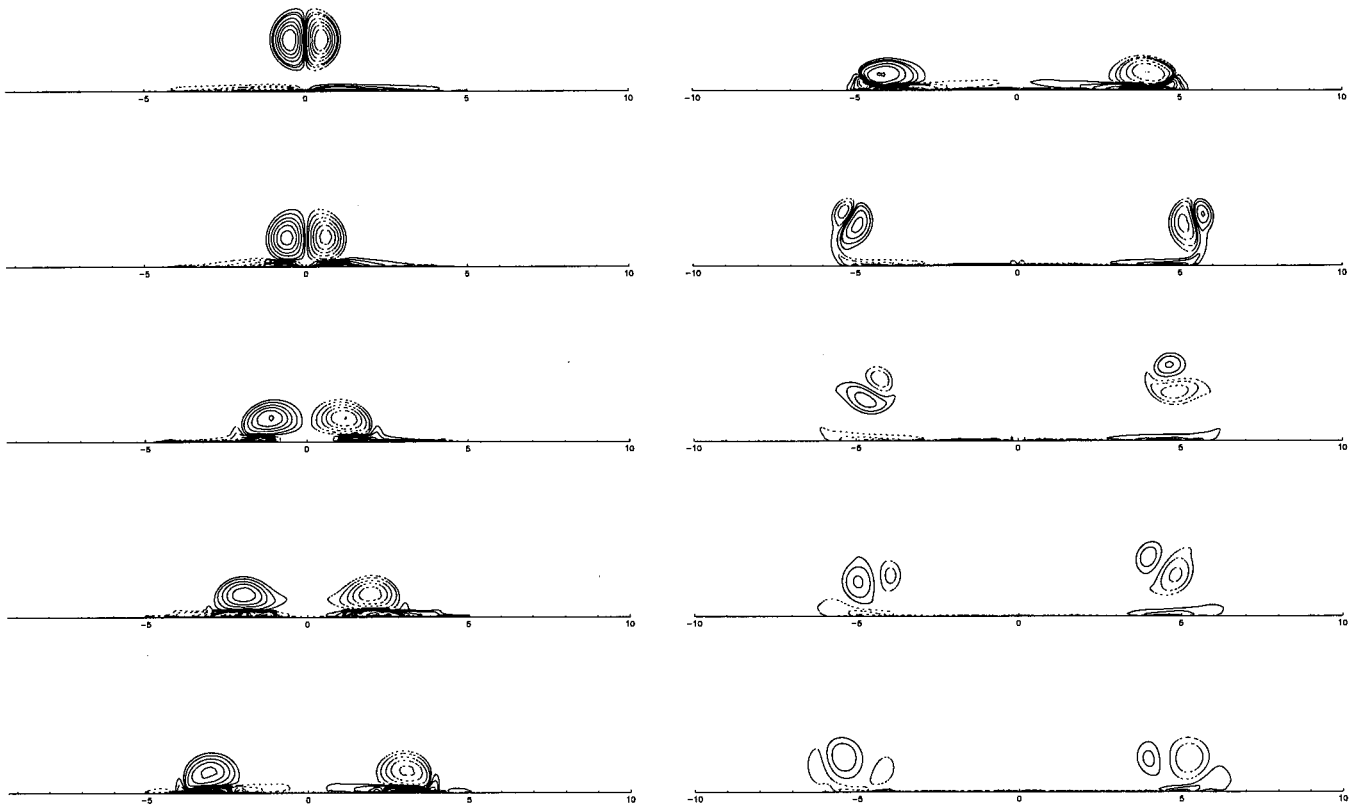

FIG. 9. Configuration 2b: *Controlled* Wall–Vortex Interaction. Contours at $T=0.0$, 0.2, 0.5, 1.0, 1.5, 2.0, 3.0, 4.0, 5.0, 6.0 (top to bottom, left to right).

ary vorticity is enhanced and the primary vortices roll over the layer of secondary vorticity, the actuator strength is diminished.

Here we make a comparison of the present active control strategy and the ''v control,'' discussed by CMK. In their simulations of control of a vortex dipole impinging at a wall, the flow velocity normal to the wall is sensed at a distance $y^+=10$ off the wall. Blowing/suction is adjusted so as to oppose this velocity. As the primary vortex descends toward the wall, the blowing/suction counteracts this motion, enhancing the generation of secondary vorticity. This secondary vorticity in turn pairs off with the primary vortex, resulting in a vortex dipole propagating parallel to the wall. It appears that the center of the newly formed dipoles is near the $y^+=10$ location. This may explain also why the control scheme is not as effective, at say $y^+=25$, as then the sensed velocity field would not be that of the dipolar structure but that of the primary vortex itself. In CMK's simulations sensors and actuators are distributed throughout the wall and the lift off of the secondary vorticity field is completely prevented. The behavior of the vorticity field is strikingly similar to the vorticity field presented here (Figs. 8 and 9) over the controlled part of the wall. This strongly suggests that CMK's control strategy and the one discussed in the previous section, are related. Although they rely on two different descriptions of the same underlying physical mechanisms,

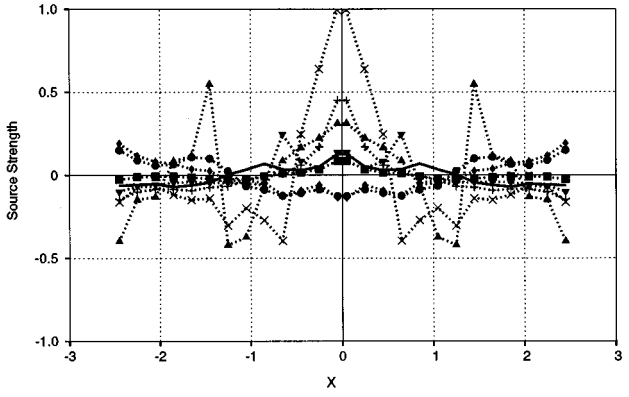

FIG. 10. Configuration 2a. For symbol captions see Fig. 6.

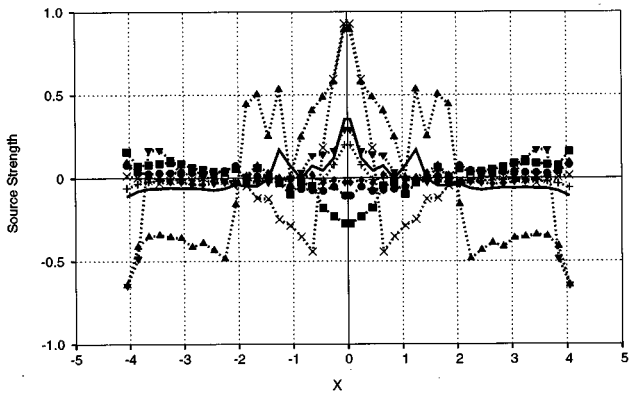

FIG. 11. Configuration 2b. For symbol captions see Fig. 6.

they induce the similar behavior to the vortical structures. The two schemes differ in the way in which they sense the vorticity field that is approaching and adjust the necessary blowing/suction at the wall. As the present adaptive control strategy relies on the sensing of the wall pressure and the calculation of the vorticity flux, it appears as more suitable to experimental applications and seems a more promising method for practical applications. The similarity of the two schemes suggests that the successful results that have been obtained using the ''v-control'' scheme in more complex flows[10,12] can be obtained more efficiently by the present strategy.

IV. CONCLUSIONS AND FUTURE WORK

An active control technique that is based on the physical mechanism of vorticity generation at the wall, is presented.

In the present scheme the vorticity flux is sensed at the wall, via the measurement of wall pressure. A simple control strategy is described that allows to calculate the strength of wall transpiration in closed form to achieve a desired wall vorticity flux. The efficiency of the control scheme is demonstrated in simulations of the model problem of a vortex dipole interactions with a wall. Using information available at the wall, the present control scheme is able to reproduce phenomena that were previously obtained computationally using off-wall information.

The implementation of the control scheme does not depend on a particular numerical method or flow configuration, making it suitable for practical applications. The simplicity of the technique and the explicit relationship between sensor and actuator outputs allows one to concentrate on issues such as devising strategies for optimal sensor and actuator placement. It may also be efficiently implemented in control schemes employing large numbers of microsensors and actuators, as its computational cost is minimal. The present scheme may be easily applied to the control of a variety of wall bounded flows and it could be effective in experimental control strategies. The proposed control algorithm has been applied to the model problem of a two-dimensional vortex dipole impinging at a wall. The control scheme acts to drastically modify the behavior of the vortex wall interactions by controlling the generation of vorticity at the wall.

It must be stressed that the present two-dimensional control and uncontrolled vortex–wall interactions do not necessarily constitute an accurate model and a realistic scenario for the phenomena that could occur when the proposed control algorithm is applied to three-dimensional vorticity fields. In particular, for turbulent wall bounded flows, as it is discussed in AA and in Moin and Kim,[3] the vorticity field is strongly three dimensional and the control algorithm would need to compensate for all three components of the wall vorticity flux. The extension of the present scheme to three dimensions is straightforward and it has been implemented in the control of turbulent channel flow.[18] The results indicate unprecedented skin friction drag reduction ($\approx 40\%$) using wall only information.

Work is underway to implement the proposed control strategy to unsteady separated bluff body flows.

ACKNOWLEDGMENTS

I wish to thank Dr. Georges-Henri Cottet, Dr. Paul Durbin, and Dr. Nagi N. Mansour for several helpful suggestions on an earlier version of this paper. Computer time was provided by the NASA Ames Supercomputing Center.

[1] J. Andreopoulos and J. H. Agui, ''Wall-vorticity flux dynamics in a two-dimensional turbulent boundary layer,'' J. Fluid Mech. **309**, 45 (1996).
[2] A. V. Johansson, P. H. Alfredsson, and J. H. Haritonidis, ''Evolution and dynamics of shear-layer structures in near-wall turbulence,'' J. Fluid Mech. **224**, 579 (1987).
[3] P. Moin and J. Kim, ''The structure of vorticity fields in turbulent channel flow. Part 1. Analysis of instantaneous field and statistical correlations,'' J. Fluid Mech. **155**, 441 (1985).
[4] P. Orlandi and X. Jimenez, ''On the generation of wall friction,'' Phys. Fluids A **6**, 634 (1994).
[5] P. Moin and T. R. Bewley, ''Feedback control of turbulence,'' Appl. Mech. Rev. **47**, S3 (1994).
[6] C. Ho and Y. Tai, ''Review: MEMS and its applications for flow control,'' J. Fluids Eng. **118**, 437 (1996).
[7] L. Löfdahl, E. Kälvesten, and G. Stemme, ''Small silicon pressure transducers for space–time correlation measurements in a flat plate boundary layer,'' J. Fluids Eng. **118**, 457 (1996).
[8] J. Z. Wu, X. H. Wu, and J. M. Wu, ''Streaming vorticity flux from oscillating walls with finite amplitude,'' Phys. Fluids A **5**, 1933 (1993).
[9] M. Gad-El-Hak, ''Control of low-speed airfoil aerodynamics,'' AIAA J. **118**, 1537 (1990).
[10] C. Lee, J. Kim, D. Babcock, and R. Goodman, ''Application of neural network to turbulence control for drag reduction,'' Phys. Fluids **9**, 1740 (1997).
[11] M. J. Lighthill, *Introduction. Boundary Layer Theory*, edited by J. Rosenhead (Oxford University Press, New York, 1963), pp. 54–61.
[12] H. Choi, P. Moin, and J. Kim, ''Active turbulence control for drag reduction in wall bounded flows,'' J. Fluid Mech. **262**, 75 (1994).
[13] H. Hornung, *Vorticity Generation and Transport*, 10th Australasian Fluid Mechanics Conference, University of Melbourne, 11–15 December 1989.
[14] R. L. Panton, *Incompressible Flow* (Wiley, New York, 1984).
[15] P. Koumoutsakos and A. Leonard, ''High resolution simulations of the flow around an impulsively started cylinder using vortex methods,'' J. Fluid Mech. **296**, 1 (1995).
[16] P. Koumoutsakos and D. Shiels, ''Simulations of the flow normal to an impulsively started and uniformly accelerated flat plate,'' J. Fluid Mech. **328**, 177 (1996).
[17] P. Orlandi, ''Vortex dipole rebound from a wall,'' Phys. Fluids A **1429**, 75 (1990).
[18] P. Koumoutsakos, ''Active control of turbulent channel flow, using wall-only information,'' in preparation.